WM36

19th International Symposium of Ballistics, 7–11 May 2001, Interlaken, Switzerland

COMPUTER SIMULATION OF SHAPED CHARGE JET FRAGMENTATION

Hans E. V. Karlsson

Saab Bofors Dynamics AB, S-631 87 Eskilstuna, Sweden

An AUTODYN-2D Euler processor was used to perform a computer simulation of a Shaped Charge detonation, including formation, elongation and fragmentation of the jet, all in the same simulation. Three degrees of fineness were used for the Euler grid, as were single and double precision. Five copper models were used for the liner material, of which one was hydrodynamic without material strength, and the others with a yield strength. Jet fragmentation was achieved in the latter case, which appears to be due to a combination of a numeric, non-physical interference and the yield strength of the liner material. In physical reality this may be the equivalent of a slight geometric imperfection in the liner or the charge in general, plus a strength characteristic for the liner material.

INTRODUCTION

When a shaped charge detonates a metal jet is created that elongates increasingly owing to the velocity gradient in the jet. The penetration capability of the jet, in steel armour for example, thus increases to a corresponding degree until the jet has fragmented completely. Fragmentation thus limits the maximum penetration of the jet.

This report discloses the computer simulations of the detonation of a shaped charge and the formation, elongation and fragmentation of the jet, which constitutes major progress – mainly thanks to developments in software – since the paper in Ref. [1]. Whether the computed jet fragmentation is physically correct, or is caused by some numerical phenomenon, is also discussed.

METHOD OF COMPUTATION

Rotation symmetrical simulations were performed using the computer program AUTODYN-2D v.3.1.14 (single precision) and v.4.1.13c-DP (double precision) with a compact, periphery-initiated shaped charge with a length to diameter ratio ≈1. The explosive (LX14, JWL) and the copper liner were modelled in Euler, and the charge casing and aft closure, etc made of aluminium alloy were modelled in Lagrange. As the shaped

charge jet gradually became longer, the Euler grid was also extended. Five material models using data from AUTODYN's directory were used for copper, see Table 1. Three degrees of fineness were selected for the Euler grid as disclosed in Table 2 that also provides an overview of the simulations performed.

Table 1. Material models used for copper. EOS = equation of state.

Material model	EOS	Strength model	Failure model	Erosion model
Hydrodynamic	shock	none (hydro)	none	none
Hull	shock	piecewise linear	none	none
Steinberg-Guinan	shock	Steinberg-Guinan	none	none
Johnson-Cook	linear	Johnson-Cook	none	none
Zerilli-Armstrong	linear	Zerilli-Armstrong	none	none

Table 2. Overview of simulations performed. Data for the Euler grid at start, t = 0 μs.

Simulation	Program version	Material model	ΔX_{total} (mm)	I_{total}	$\Delta Y_{central}$ (mm)	$J_{central}$	J_{total}	Fig. no.
JU03	v.3.1.14	Hydrodynamic	0.25	801	0.1	51	301	1
JS03	v.3.1.14	Hull	0.25	801	0.1	51	301	2
JT03	v.3.1.14	Johnson-Cook	0.25	801	0.1	51	301	3
JQ03	v.3.1.14	Zerilli-Armstrong	0.25	801	0.1	51	301	4
JR03	v.3.1.14	Steinberg-Guinan	0.25	801	0.1	51	301	---
JD7	v.4.1.13c-DP	Hydrodynamic	0.25	721	0.1	51	301	5
JD3	v.4.1.13c-DP	Hull	0.25	721	0.1	51	301	6
JD8	v.4.1.13c-DP	Hydrodynamic	0.5	361	0.2	26	201	7
JD5	v.4.1.13c-DP	Hull	0.5	361	0.2	26	201	8
JD9	v.4.1.13c-DP	Hydrodynamic	1.0	181	0.4	14	201	9
JD6	v.4.1.13c-DP	Hull	1.0	181	0.4	14	201	10

RESULTS

The results from ten of the simulations at time t = 120 μs, which is the same for all cases, is shown in Figs. 1 to 10 as per Table 2. For the sake of clarity the image of the shaped charge jet has been magnified and divided into five equally long parts. The scale and the minimum and maximum values of the X-axis are the same for all simulations.

The two simulations with the hydrodynamic copper model, Figs. 1 and 5 (single and double precision respectively), and the finely divided Euler grid gave a jet with varying diameter but no fragmentation. The most peripheral parts of the computational model with the outer part of the slug were eliminated at a later stage to reduce computation time. This fact did not affect the jet in any other way.

Figs. 2 to 4 show that the introduction of a strength model for the copper results in fragmentation of the jet. The Steinberg-Guinan model, which cannot be shown here for lack of space, showed a similar result. In all cases the tailmost part of the jet displays a diffuse appearance.

Figs. 5 and 6 in comparison with Figs. 1 and 2 respectively show that transition to double precision did not entail any significant change in the appearance of the jet, e.g. the diffuse fragments in the tail of the jet did not change appreciably.

Figs. 5 to 10 show that transition from a hydrodynamic copper model to a copper model with material strength results in fragmentation even when the grid of the Euler model is made coarser. However, the number of fragments is reduced and, further, the fragments in the tail of the jet become less diffuse the coarser the grid becomes.

DISCUSSION

The results from the computer simulations of a shaped charge detonation and the formation, elongation and fragmentation of the jet show that:

– the hydrodynamic copper model gives variations in diameter but no fragmentation
– copper models with material strength give fragmentation
– the finest Euler grid clearly gives fewer fragments than the real shaped charge
– a coarser Euler grid gives even fewer fragments
– a coarser Euler grid gives less diffuse fragments in the tail part of the jet.

CONCLUSIONS

The fragmentation of the shaped charge jet obtained in the computer simulations disclosed herein may derive from a combination of two factors:

1) A numerical perturbation caused by the copper liner at detonation moving obliquely inwards through the rectangular Euler grid.
2) The copper liner has a certain material strength.

As (1) is a non-physical phenomenon the fragmentation displayed in the simulations is also non-physical. However, it is conceivable that (1) in reality, for example, might correspond to some slight geometrical discrepancy in the liner, or in the charge in general, that has the same effect. Ref. [2] also shows that a very small local variation in diameter in a shaped charge jet that elongates gives rise to necking of the jet. Necking can subsequently lead to fragmentation.

REFERENCES

1. H. E. V. Karlsson, "Computer Calculations of Wide-Angle Shaped Charge Liner Acceleration and Deformation", *Proceedings of the 1st International Symposium on Ballistics*, IV: 257–270, 1974
2. L. Zernow, "An Overview of the New Insights into Jet Formation and Particulation, Provided by Examination of Recovered Jet Particles"", *Proceedings of the 15th International Symposium on Ballistics*, Vol. 2, WM2, 129–141, 1995

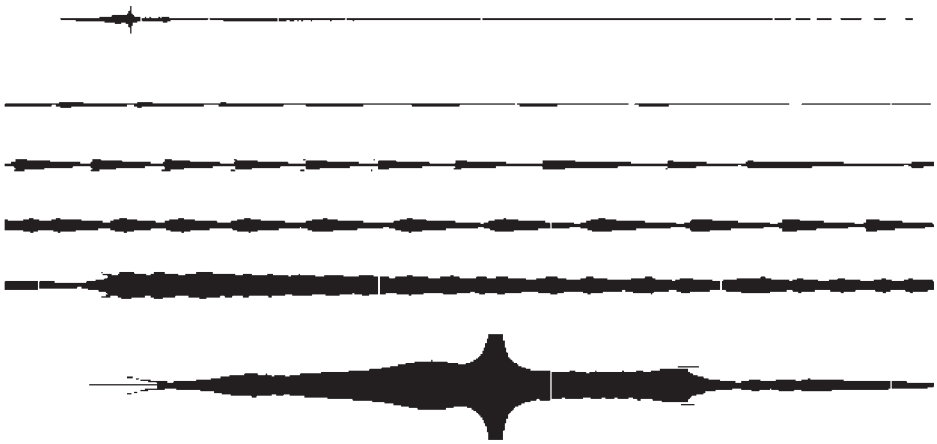

Figure 1. Jet at t = 120 μs. Simulation JU03, finest Euler grid, hydrodynamic copper model. Complete jet shown uppermost, and then divided into five equally long parts and magnified.

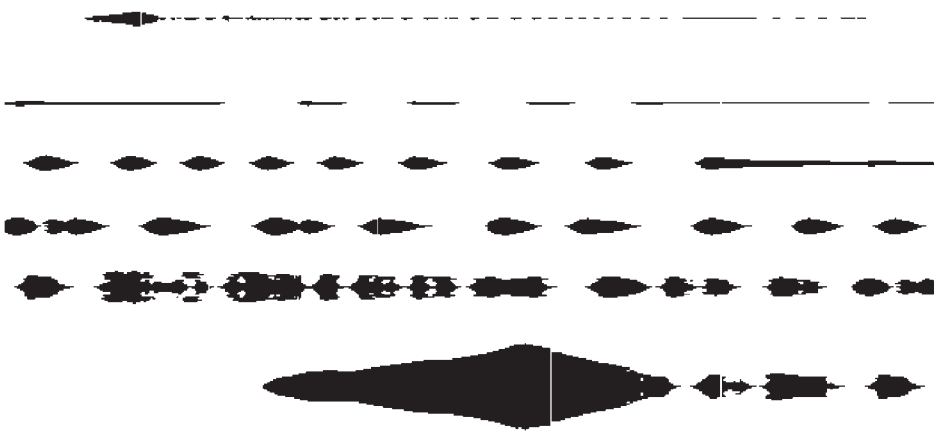

Figure 2. Jet at t = 120 μs. Simulation JS03, finest Euler grid, hull copper model. Complete jet shown uppermost, and then divided into five equally long parts and magnified.

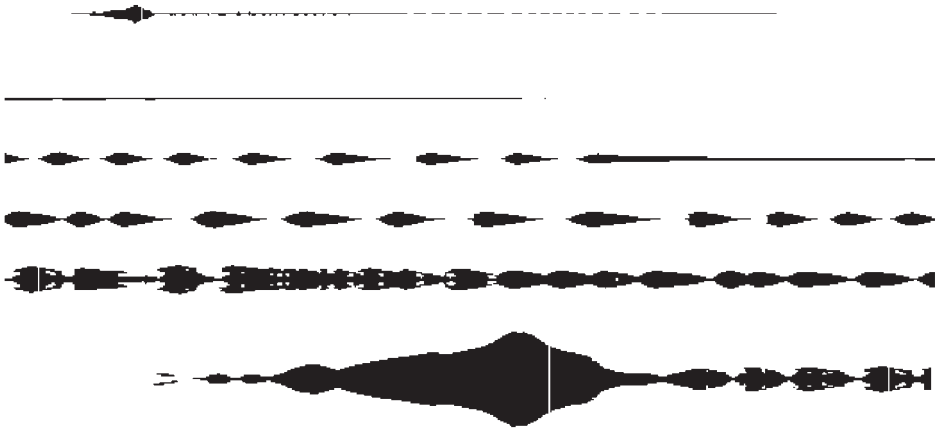

Figure 3. Jet at t= 120 μs. Simulation JT03, finest Euler grid, Johnson-Cook copper model. Complete jet shown uppermost, and then divided into five equally long parts and magnified.

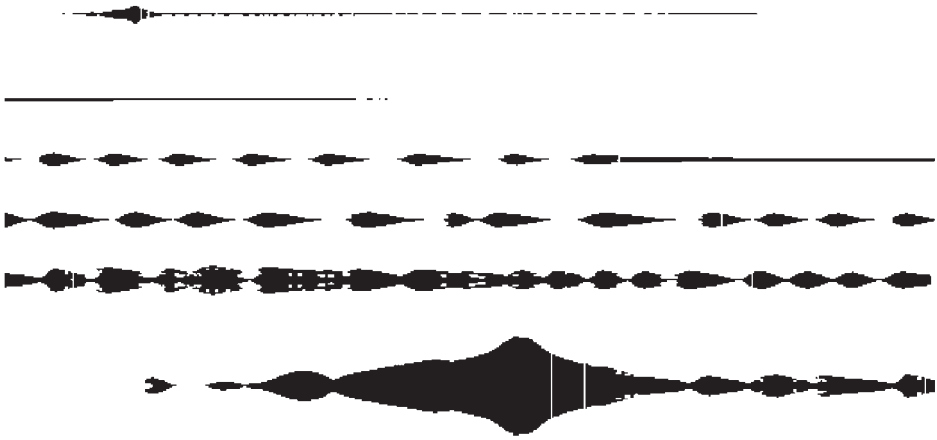

Figure 4. Jet at t= 120 μs. Simulation JQ03, finest Euler grid, Zerilli-Armstrong copper model. Complete jet shown uppermost, and then divided into five equally long parts and magnified.

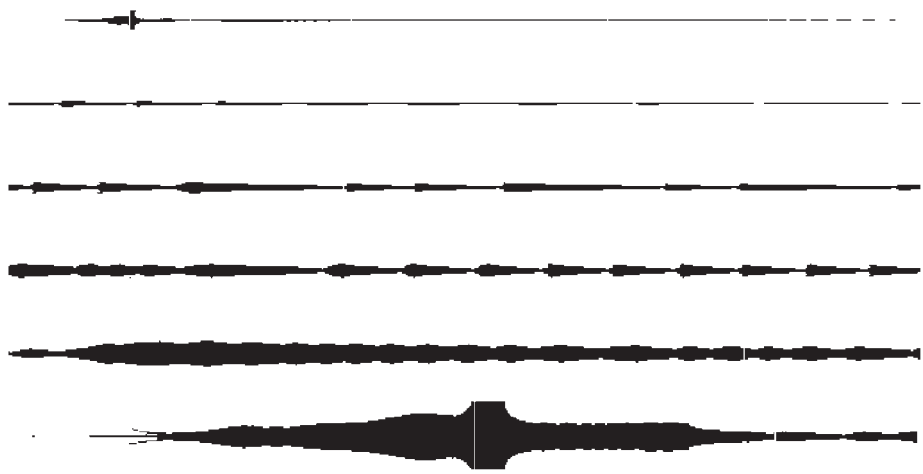

Figure 5. Jet at t= 120 μs. Simulation JD7, finest Euler grid, hydrodynamic copper model. Double precision. Complete jet shown uppermost, and then divided into five equally long parts and magnified.

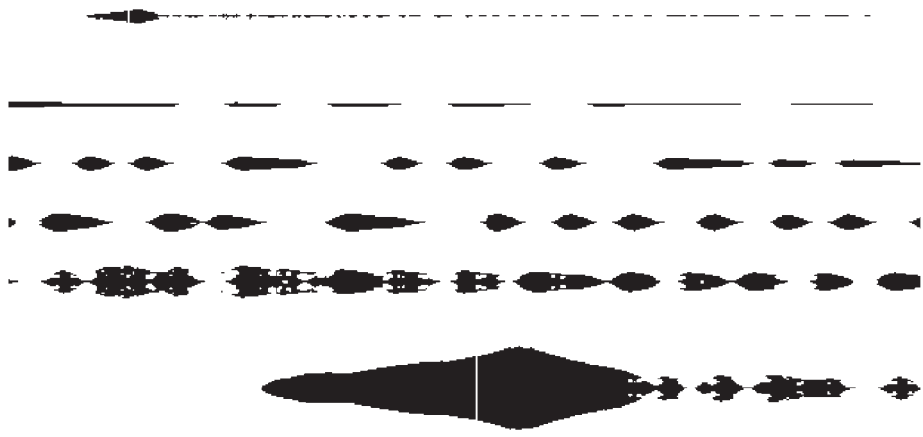

Figure 6. Jet at t= 120 μs. Simulation JD3, finest Euler grid, Hull copper model. Double precision. Complete jet shown uppermost, and then divided into five equally long parts and magnified.

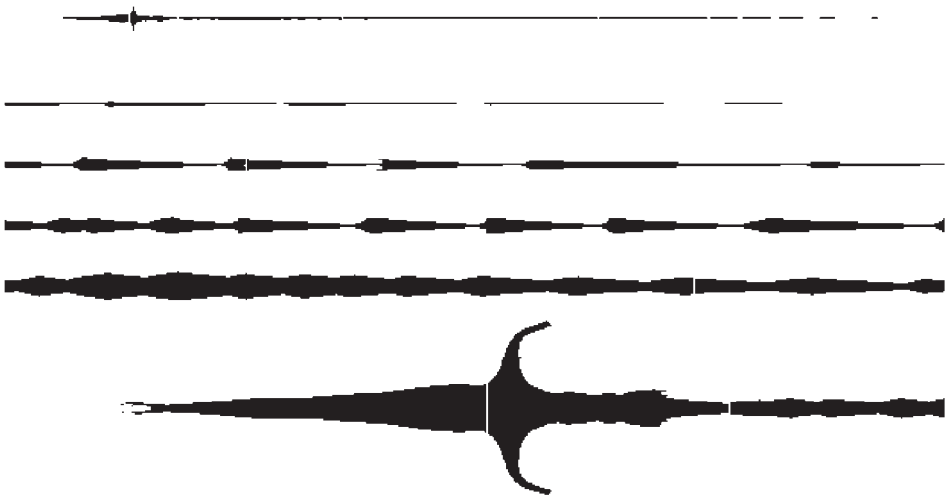

Figure 7. Jet at t= 120 μs. Simulation JD8, medium Euler grid, hydrodynamic copper model. Double precision. Complete jet shown uppermost, and then divided into five equally long parts and magnified.

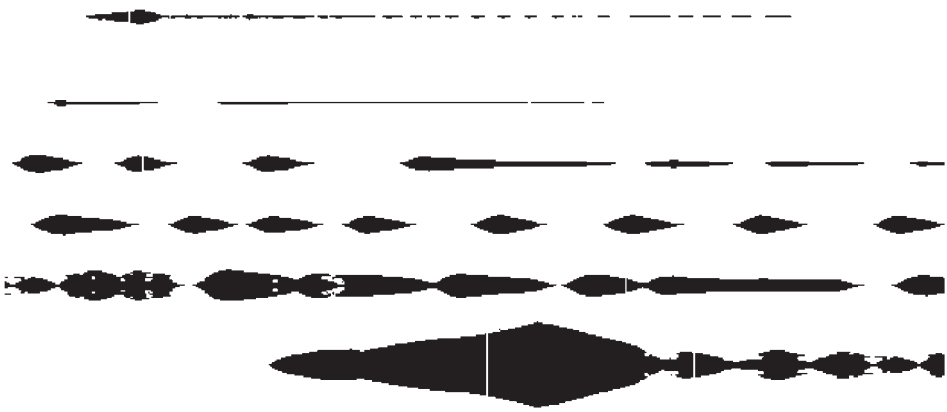

Figure 8. Jet at t= 120 ms. Simulation JD5, medium Euler grid, Hull copper model. Double precision. Complete jet shown uppermost, and then divided into five equally long parts and magnified.

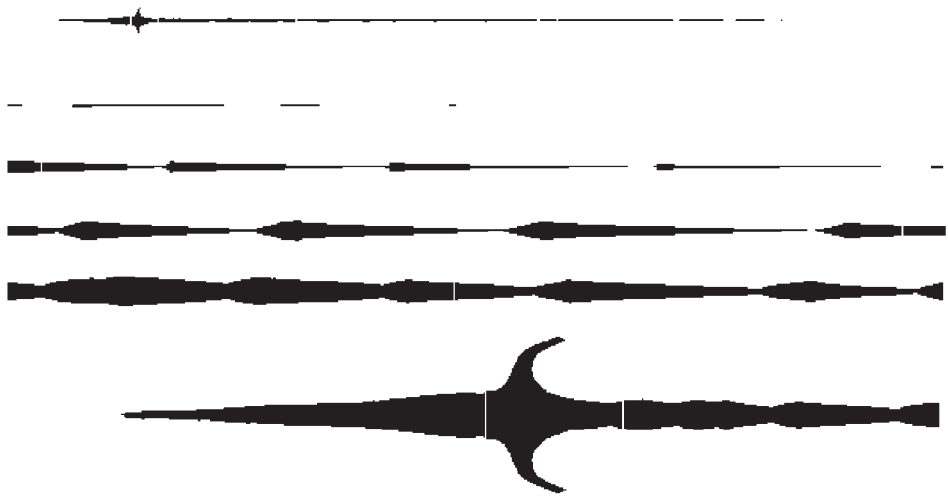

Figure 9. Jet at t= 120 μs. Simulation JD9, coarse Euler grid, hydrodynamic copper model. Double precision. Complete jet shown uppermost, and then divided into five equally long parts and magnified.

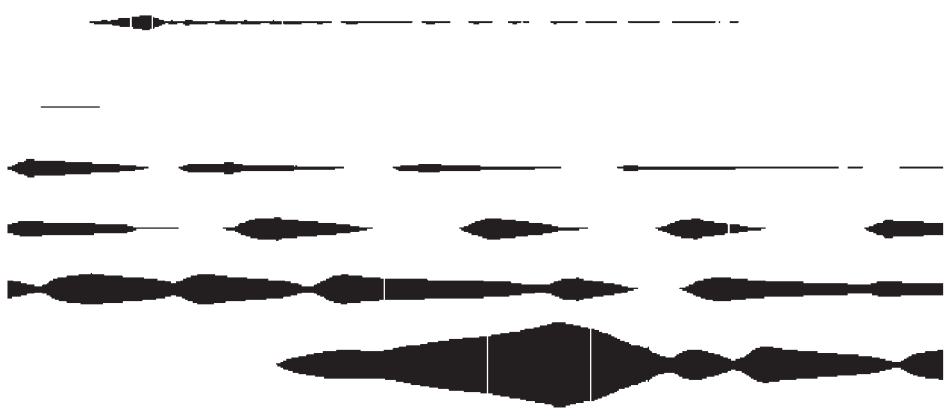

Figure 10. Jet at t= 120 μs. Simulation JD6, coarse Euler grid, Hull copper model. Double precision. Complete jet shown uppermost, and then divided into five equally long parts and magnified.